[Review] doi: 10.3866/PKU.WHXB201511272 www.whxb.pku.edu.cn

固态Photo-CIDNP效应

王孝杰[1,*] THAMARATH Smitha Surendran[2,3] ALIA A.[2,3,4]
BODE Bela E.[5] MATYSIK Jörg[2,3,*]

([1]国防科技大学理学院化学与生物学系，长沙 410073；[2]莱比锡大学分析化学研究所，莱比锡 04103，德国；[3]莱顿大学化学院，莱顿 2300RA，荷兰；[4]莱比锡大学医学物理与生物物理研究所，莱比锡 D-04107，德国；[5]圣安德鲁斯大学化学与生物医学研究院，圣安德鲁斯 KY16 9ST，苏格兰)

摘要：光化学诱导动态核极化(photo-CIDNP)是一种在光照条件下由于产生非玻尔兹曼核自旋极化而使核磁共振(NMR)波谱信号强度发生明显变化的效应。这种效应在液体NMR中已为人所熟知，并通过经典的自由基对机理得到解释。固态photo-CIDNP效应发现的较晚，本文介绍了在光合反应中心及蓝光受体中发现的固态photo-CIDNP效应，详细阐述了固态photo-CIDNP效应产生的自由基对自旋动力学的机理，包括三旋混合(TSM)、衰变差异(DD)和弛豫差异(DR)，重点介绍了类球红杆菌光合反应中心固态photo-CIDNP效应的磁场依赖性，这种场依赖性在同一分子中的不同核之间表现出明显的差异。本文综述了固态photo-CIDNP效应的现象、理论及其磁场依赖特性的最新进展。

关键词：光化学诱导动态核极化；魔角旋转；核磁共振；自由基对；自旋化学
中图分类号：O646.8

The Solid-State Photo-CIDNP Effect

WANG Xiao-Jie[1,*] THAMARATH Smitha Surendran[2,3] ALIA A.[2,3,4]
BODE Bela E.[5] MATYSIK Jörg[2,3,*]

([1]*Department of Chemistry and Biology, College of Science, National University of Defense Technology, Changsha 410073, P. R. China*; [2]*Institut für Analytische Chemie, Universität Leipzig, Linnéstr. 3, 04103 Leipzig, Gemany*; [3]*Leiden Institute of Chemistry, Einsteinweg 55, 2300 RA Leiden, The Netherlands*; [4]*Institute of Medical Physics and Biophysics, University of Leipzig, D-04107 Leipzig, Germany*; [5]*EaStCHEM School of Chemistry and Biomedical Sciences Research Complex, University of St Andrews, St Andrews, KY16 9ST, Scotland*)

Abstract: Photochemically induced dynamic nuclear polarization (photo-CIDNP) is an effect that produces non-Boltzmann nuclear spin polarization, which can be observed as a modification of signal intensity in nuclear magnetic resonance (NMR) spectroscopy. The effect is well known in liquid-state NMR, where it is explained most generally by the classical radical pair mechanism (RPM). In the solid-state, additional mechanisms are operative in the spin-dynamics of radical pairs, such as three-spin mixing (TSM), differential decay (DD) and differential relaxation (DR). The observed solid-state photo-CIDNP effect is strongly magnetic field dependent, and this field-dependence is well distinguished for the various nuclei. Here, we provide an account of the phenomenology, theory and properties of the magnetic field dependence of the solid-state photo-CIDNP effect.

Key Words: Photo-CIDNP; Magic angle spinning; Nuclear magnetic resonance; Radical pair; Spin chemistry

Received: September 21, 2015; Revised: November 26, 2015; Published on Web: November 27, 2015.

*Corresponding authors. WANG Xiao-Jie, Email: yj605@126.com; Tel: +86-13308490803. MATYSIK Jörg, joerg.matysik@uni-leipzig.de.

The project was supported by the Netherlands Organization for Scientific Research (NWO) (713.012.001).
荷兰科学研究组织(NWO) (713.012.001)资助项目

1 Introduction

Photochemically induced dynamic nuclear polarization (photo-CIDNP) is an effect that produces non-Boltzmann nuclear spin polarization that can be observed by nuclear magnetic resonance (NMR) spectroscopy as enhanced absorptive (positive) or emissive (negative) signals. The photo-CIDNP effect is produced during a chemical reaction, therefore, the relevant mechanistic chemistry studies can take advantage of this effect.

The effect is well known in liquid-state NMR where it is explained most generally by the classical radical pair mechanism (RPM)[1,2]. However, due to restrictions on molecular weight of sample in liquid NMR and the necessity of molecular diffusion, the applicability of the liquid-state photo-CIDNP effect is limited by molecular weight and viscosity[3]. These limits can be overcome by the solid-state photo-CIDNP effect.

The solid-state photo-CIDNP effect was observed for the first time in 1994 by McDermott's group[4] in frozen and quinone-blocked bacterial reaction centers (RCs) of ^{15}N-labeled *Rhodobacter* (*R.*) *sphaeroides* by magic-angle spinning (MAS) NMR. Subsequent studies[5,6] found that the effect allows for signal enhancement of factors of several 10000 s. Such strong signal enhancement allows for example selectively observing photosynthetic cofactors forming radical-pairs at nanomolar concentrations in membranes, cells, and even in entire plants[7]. Due to the long ^{13}C relaxation time in solids, the nuclear polarization of subsequent photocycles can be accumulated in continuous illumination experiments making photo-CIDNP MAS NMR a sensitive analytical tool for studying radical pairs[8–10].

2 Solid-state photo-CIDNP effect

2.1 Phenomenon

The solid-state photo-CIDNP effect was observed for the first time in 1994; meanwhile the effect has been shown in various other RCs[11–13]. Most solid-state photo-CIDNP research has been carried out on the purple bacterium *R. sphaeroides* as a model organism for bacterial photosynthesis[14,15]. Our group measured the ^{13}C MAS NMR spectra of quinone depleted RCs of *R. sphaeroides* wild-type (WT) and of the carotenoid-less mutant R26 in the dark and under illumination, respectively. The result is shown in Fig.1. In the spectrum obtained in the dark, the expected broad protein resonances appear. Under illumination with continuous white light, several strong light-induced signals appeared. These signals are generated due to the solid-state photo-CIDNP effect.

The solid-state photo-CIDNP effect has been observed in all natural photosynthetic RCs studied so far[13]. Using this effect for enhancing NMR signals, a series of studies of photosynthetic RCs have been carried out. The photo-CIDNP MAS NMR has become an important means in mechanistic research of photosynthetic charge separation. Despite great efforts, experiments on systems other than natural photosynthetic RCs were unsuccessful for a long time. It has been discussed whether the effect might be confined to natural photosynthetic RCs.

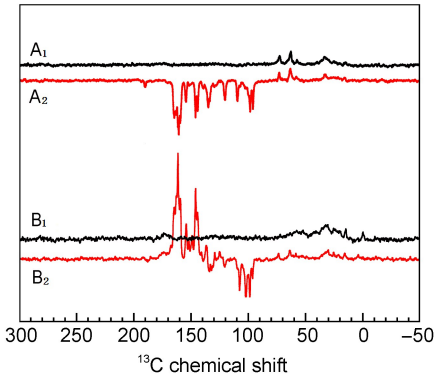

Fig.1 ^{13}C MAS NMR spectra of quinone depleted RCs of *R. sphaeroides* WT (A_1, A_2) and of the carotenoid-less mutant R26 (B_1, B_2) in the dark (A_1, B_1) and under continuous illumination with white light (A_2, B_2) at 4.7 T[16]

The spectra were obtained at 235 K under a MAS frequency of 8 kHz under ^{1}H decoupling.

Recently, we observed the solid-state photo-CIDNP effect in a rather different, nonphotosynthetic protein, a mutant of the blue-light photoreceptor phototropin (LOV1-C57S)[17]. This is the first observation of this effect in a non-photosynthetic system, this demonstrated that the solid-state photo-CIDNP effect is not a peculiarity of photosynthetic systems. The result is shown in Fig.2.

Since the occurrence of the solid-state photo-CIDNP effect had been limited to photosynthetic RCs for a long time, this method has not attracted much attention, although its capacity to enhance NMR signals dramatically has been recognized. Our observation of the solid-state photo-CIDNP effect in phototropin allows us to assume that the effect can arise in other photoactive electron-transfer proteins too. Induction of the effect in artificial diads would certainly allow evolving a generally applicable method for signal enhancement in NMR.

2.2 Fundamentals

The cyclic spin-chemical processes producing such high nuclear polarizations are now understood[18] for a spin-correlated radical pair interacting with a single nuclear spin in quinone depleted RCs

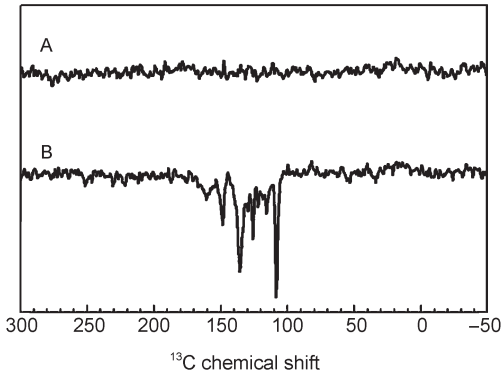

Fig.2 ^{13}C MAS NMR spectra of phototropin LOV1-C57S obtained at a magnetic field of 2.3 T in the dark (A) and under continuous illumination with white light (B)[17]

The spectra were obtained at 235 K under a MAS frequency of 8 kHz under ^{1}H decoupling.

of *R. sphaeroides*. Under illumination, RCs form radical pairs with the primary electron donor P, the so-called "special pair" of two bacteriochlorophylls (BChl), as radical cation and the primary electron acceptor Φ, a bacteriopheophytin (BPhe), as radical anion (Scheme 1).

The radical pair mechanism (RPM)[19,20], well established in liquid-state photo-CIDNP, is active in spin-sorting, i.e., enriching one nuclear spin state in one of the two decay channels of the radical pair and depleting it in the other. Since the product state in Scheme 1 is identical for both branches of the radical-pair decay, in steady-state experiments using continuous illumination the process of spin sorting does not lead to observable net nuclear polarization: the polarizations arising from the two channels exactly cancel.

Time-resolved experiments (Fig.3, spectrum C), however, are able to observe the spin-sorting by the RPM. Fig.3 shows the evolution of signal intensity on microsecond timescale. Initially positive (absorptive) transient nuclear polarization occurs and is visible up to 10 μs. This initial phase is due to the RPM and shows selectively the enriched nuclear polarization on the singlet decay pathway. This polarization is only transiently visible, in this case because the nuclear polarization occurring on the triplet decay pathway is shifted and broadened beyond detection by the nearby paramagnetic carotenoid triplet[21]. After the decay of the transient nuclear polarization from the singlet decay channel, a new pattern

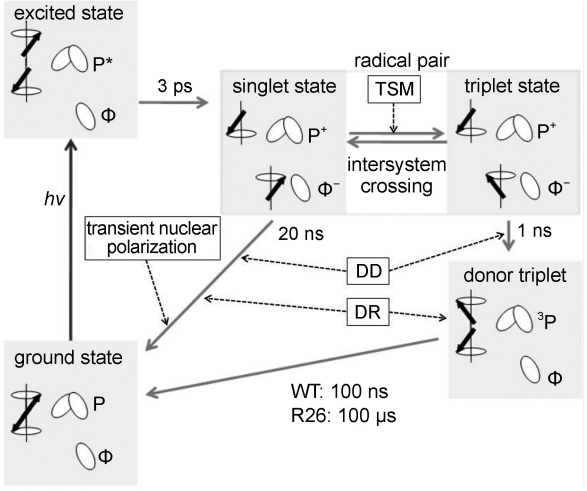

Scheme 1 Kinetics and spin dynamics of solid state photo-CIDNP in *R. sphaeroides* WT and R26 RCs

Upon illumination and fast electron transfer from an excited singlet state, a radical pair is formed in a pure singlet state having electron two-spin order of unity. The radical pair is formed by a radical cation at the two donor BChls (special pair, P) and a radical anion on the BPhe acceptor cofactor (Φ) of the active branch. The chemical fate of the radical pair depends on its electronic spin state: while the singlet state (*S*) is allowed to recombine, for the triplet state (*T*) a direct recombination to the ground state is spin-forbidden and a donor triplet (^{3}P) is formed instead. The lifetime of ^{3}P depends on the relaxation channels provided by the environment. Therefore it is short in WT RCs having a near-by carotenoid and significantly longer in the carotenoid-less mutant R26. Mechanisms building up photo-CIDNP under steady-state conditions are three-spin mixing (TSM), differential decay (DD), and differential relaxation (DR). Transient nuclear polarization could be observed in time-resolved experiments.

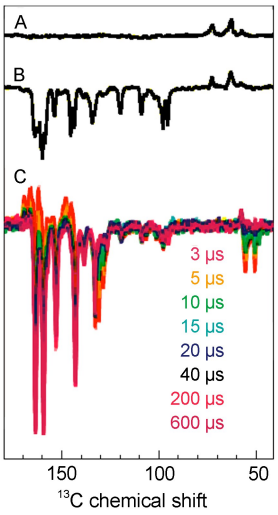

Fig.3 ^{13}C MAS NMR spectra of WT RCs measured in the dark (A), under continuous illumination (B), and after a nanosecond-laser flash (C)[22]

The sample is selectively ^{13}C isotope labelled at the tetrapyrrole cofactors (4-Ala label pattern). The laser pulse length is ~10 ns and the wavelength 532 nm.

occurs, showing an entirely negative (emissive) envelope on the 100 μs timescale. Equilibration of the polarization by spin diffusion on ms timescale leads to the all-emissive steady-state intensity pattern (Fig.3, spectrum B)[22].

The all-emissive steady-state pattern is caused by two solid-state mechanisms, called the three-spin mixing (TSM)[23,24] and the differential decay (DD)[25].

In the electron-electron-nuclear TSM mechanism, the symmetry of the coherent spin evolution in the correlated radical pair is broken by state mixing due to electron-electron coupling and pseudosecular hyperfine coupling (hfc). State mixing is maximized at the double matching condition $2|\Delta\Omega| = 2|\omega_I| = |A|$, i.e., the difference of the electron Zeeman frequencies ($\Delta\Omega$), the nuclear Zeeman frequency (ω_I) and the secular part of the hyperfine interaction (A) must match.

In the DD mechanism, the symmetry between the singlet and triplet decay pathways is broken by different lifetimes of the *S* and of the T_0 states of the radical pair and by pseudosecular hyperfine coupling. In this case, only a single matching of interactions $2|\omega_I| = |A|$ is required and the difference of singlet and triplet radical pair lifetimes must be of the order of the inverse hfc.

During the radical pair evolution the TSM and DD mechanisms in RCs of *R. sphaeroides* WT lead to a set of entirely emissive (negative) signals, whose relative intensity encodes information on spin density distribution in the radical pair state[26]. The sign of the signal depends on the signs of the secular hyperfine coupling and of the ***g*** tensor difference[27].

In RCs having a long donor triplet lifetime as in the carotenoid-less mutant R26 of *R. sphaeroides*, contributions from a third mechanism have been observed[28]. Here, the polarization generated by RPM, which has the same amplitude and opposite signs in the singlet and triplet decay branches and thus usually cancels in steady state experiments, is partially maintained[29,30] due to different

longitudinal nuclear relaxation in the two branches. In the solid state this has been termed the differential relaxation (DR) mechanism to emphasize that RPM polarization is modified according to the different relaxation rates for different nuclei[27]. This mechanism explains the differences between photo-CIDNP MAS NMR spectra of RCs of *R. sphaeroides* WT and R26[16]. The DR mechanism relies on enhanced nuclear relaxation in the triplet branch, which is in turn caused by fluctuations of the anisotropic hyperfine couplings of these nuclei to the donor triplet (^{3}P) state. Therefore, relative line intensity in this case also encodes information on the electron spin density distribution in the ^{3}P state[16]. This mechanism can also occur under liquid-state conditions and is also called "cyclic reaction" mechanism.

2.3 Magnetic field dependence

It was found that the solid-state photo-CIDNP effect has a feature of magnetic field dependence. The effect is closely related to the strength of the external magnetic field. The occurrence of the effect is limited to certain field windows, and the maximum intensity enhancement occurs when the matching conditions are fulfilled.

From RCs of *R. sphaeroides*, the best investigated photosynthetic RC, the field-dependence of the amplitude of the solid-state photo-CIDNP effect has been studied in the range from 1.4 to 17.6 T in WT and R26, respectively (Figs.4−7)[16]. At fields below 2.4 T, our hardware does not allow for ^{1}H decoupling. To compare the effect of decoupling on the spectra, we measured ^{1}H-coupled and decoupled spectra for both samples at this field. The comparison shows that in particular the signals around 100 originating from methine bridge carbons, which are directly bound to a proton, are broadened beyond detection in the ^{1}H-coupled spectra while the other signals just broaden substantially.

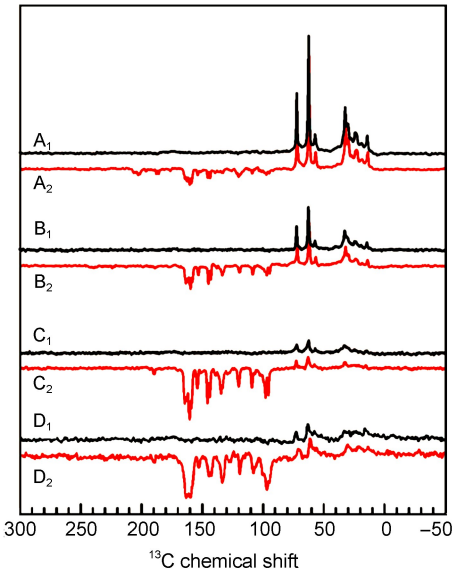

Fig.4 ^{13}C MAS NMR spectra of quinone depleted RCs of *R. sphaeroides* WT in the dark (A_1−D_1) and under illumination (A_2−D_2) at 17.6 T (A_1, A_2), 9.4 T (B_1, B_2), 4.7 T (C_1, C_2), and 2.4 T (D_1, D_2)[16]

The spectra were obtained at 235 K under a MAS frequency of 8 kHz under ^{1}H decoupling.

Within the entire field regime, the intensity patterns are different between spectra of WT and R26 RCs. While the first are entirely emissive spectra, in the latter both emissive and absorptive lines occur. The optimum for the spectral resolution is reached at about 4.7 T since at 2.4 T the spectral dispersion becomes too poor. WT RCs show the maximum enhancement around 2.4 T. On the other hand, for R26 RCs the maximum enhancement is not reached at 1.4 T and the ratio between positive and negative signals is changed strongly in favor of the first. For 1.4 T, we estimate an enhancement factor of at least 80000 due to the DR mechanism. Experiments at even lower fields would require a field cycling system to avoid further loss of resolution.

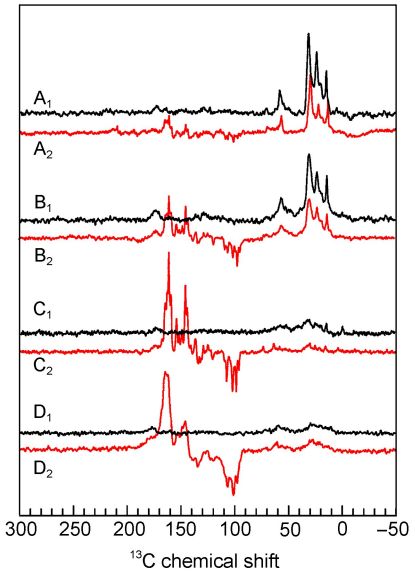

Fig.5 ^{13}C MAS NMR spectra of quinone depleted RCs of *R. sphaeroides* R26 in the dark (A_1−D_1) and under illumination (A_2−D_2) at 17.6 T (A_1, A_2), 9.4 T (B_1, B_2), 4.7 T (C_1, C_2), and 2.4 T (D_1, D_2)[16]

The spectra were obtained at 235 K under a MAS frequency of 8 kHz under ^{1}H decoupling.

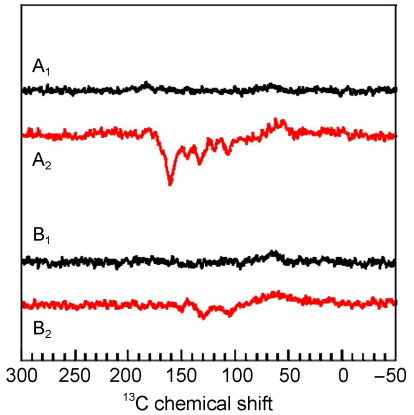

Fig.6 ^{13}C MAS NMR spectra of quinone depleted RCs of *R. sphaeroides* WT in the dark (A_1, B_1) and under illumination (A_2, B_2) at 2.4 T (A_1, A_2) and 1.4 T (B_1, B_2)[16]

The spectra were obtained at 235 K under a MAS frequency of 8 kHz without ^{1}H decoupling.

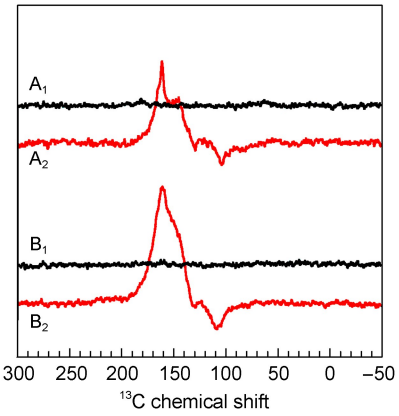

Fig.7 ^{13}C MAS NMR spectra of quinone depleted RCs of *R. sphaeroides* R26 in the dark (A_1, B_1) and under illumination (A_2, B_2) at 2.4 T (A_1, A_2) and 1.4 T (B_1, B_2)[16]

The spectra were obtained at 235 K under a MAS frequency of 8 kHz without ^{1}H decoupling.

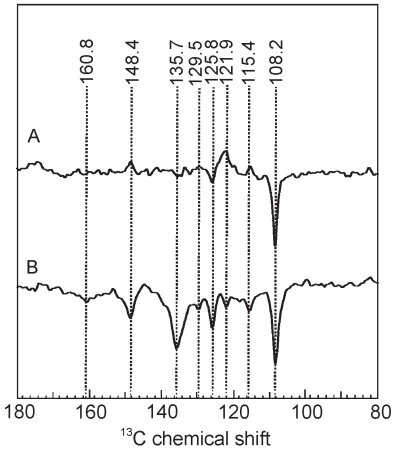

Fig.8 ^{13}C MAS NMR spectra of phototropin LOV1-C57S under illumination at magnetic fields of 4.7 T (A) and 2.4 T (B)[31]

After the first observation[17] of the solid state photo-CIDNP effect in LOV1-C57S, we also studied[31] the effect of different intensities of magnetic fields. The results show that the solid-state photo-CIDNP effect produced by the non-photosynthetic protein also has magnetic field dependence.

As can be seen from Fig.8, the chemical shifts of the main signals are the same in both spectra that measured in different magnetic fields. It shows that the radical pair formed in the composition is the same in both experiments. In contrast to the entirely emissive (negative) peaks in the photo-CIDNP MAS NMR spectra observed at 2.4 T, the light-induced ^{13}C NMR peaks at 4.7 T show mixed absorptive/emissive enhancement pattern. It shows a strong magnetic field effect on the solid-state photo-CIDNP effect.

This large difference in magnetic field dependence for different nuclei reflects the large variety of hyperfine factors found in this comparable small-sized radical pair.

3 Results and prospect

The solid-state photo-CIDNP effect has the capacity to enhance NMR signals dramatically. We estimate an enhancement factor of at least 80000 in RCs of *R. sphaeroides* at 1.4 T. Our observation of the solid-state photo-CIDNP effect in phototropin demonstrated that the effect is not a peculiarity of photosynthetic systems. It can arise in other photoactive electron-transfer proteins too. The solid-state photo-CIDNP effect can be explained by three mechanisms that operative in the spin-dynamics of radical pairs such as TSM, DD, and DR. All the observed solid-state photo-CIDNP effect has a feature of magnetic field dependence. The effect is closely related to the strength of the external magnetic field. This field-dependence is well distinguished for the various nuclei.

We have seen that the solid mechanisms of the photo-CIDNP effect (TSM mechanism, DD mechanism, and DR mechanism) acting in RCs of *R. sphaeroides* show a broad maximum at high fields as it is expected for a matching mechanism. The low-field TSM theory[32] predicts the occurrence of a second broad maximum, which matches the magnetic field strength in the tens of microtesla (μT). The region is the same order of magnitude with the earth's magnetic field, which led us to speculate that solid-state photo-CIDNP effect at earth field plays a role in the magnetoreception of biological systems.

The observation of the solid-state photo-CIDNP effect in phototropin has been shown that this effect is not limited to natural photosynthetic systems. In the same way that photo-CIDNP MAS NMR has provided detailed insights into photosynthetic electron transport in RCs, we anticipate a variety of applications in mechanistic studies of other photoactive proteins. Currently, we are using the solid-state photo-CIDNP effect to research the functionality of blue-light photoreceptors. It may be possible to characterize the photoinduced electron transfer process in cryptochrome in detail. Cryptochrome (Cry) is a member of the family of flavin-containing blue-light photoreceptors. Many research results[33] support the hypothesis of light-induced spin-dynamics as source of magnetoreception and suggest cryptochrome as the magnetoreceptor. Moreover, the radical pair formed in the cryptochrome photoreaction is sensitive to much weaker magnetic fields. Nevertheless, there is still no direct evidence for the Cry-based model of avian magnetoreception. A recent review[34] proposes that it requires a new experimental analysis tool to solve this problem. photo-CIDNP MAS NMR may allow to characterize in detail the photoinduced flavin and tryptophan radicals in cryptochrome, thereby providing direct experimental means to study the related mechanism.

Acknowledgments: The authors would like to thank Prof. Gunnar Jeschke (ETH Zürich) and Dr. Tilman Kottke (Univ. Bielefeld).

References

(1) Bargon, J.; Fischer, F.; Johnson, U. Z. *Naturforsch. A* **1967,** *22*, 1551.

(2) Ward, H. R.; Lawler, R. G. *J. Am. Chem. Soc*. **1967,** *89*, 5518.

doi: 10.1021/ja00997a078

(3) Richter, G.; Weber, S.; Römisch, W.; Bacher, A.; Fischer, M.; Eisenreich, W. *J. Am. Chem. Soc.* **2005,** *127*, 17245. doi: 10.1021/ja053785n

(4) Zysmilich, M.; McDermott, A. *J. Am. Chem. Soc.* **1994,** *116*, 8362. doi: 10.1021/ja00097a052

(5) Prakash, S.; Alia; Gast, P.; de Groot, H. J. M.; Jeschke, G.; Matysik, J. *J. Am. Chem. Soc.* **2005,** *127*, 14290. doi: 10.1021/ja054015e

(6) Prakash, S.; Alia; Gast, P.; de Groot, H. J. M.; Matysik, J.; Jeschke, G. *J. Am. Chem. Soc.* **2006,** *128*, 12794. doi: 10.1021/ja0623616

(7) Janssen, G. J.; Daviso, E.; van Son, M.; de Groot, H. J. M.; Alia, A.; Matysik, J. *Photosynth. Res.* **2010,** *104*, 275. doi: 10.1007/s11120-009-9508-1

(8) Roy, E.; Alia, A.; Gast, P.; van Gorkom, H. J.; de Groot, H. J. M.; Jeschke, G.; Matysik, *J. Biochem. Biophys. Acta* **2007,** *1767*, 610. doi: 0.1016/j.bbabio.2006.12.012

(9) Prakash, S.; Alia, A.; Gast, P.; de Groot, H. J. M.; Jeschke, G.; Matysik, J. *Biochemistry* **2007,** *46*, 8953. doi: 10.1021/bi700559b

(10) Roy, E.; Rohmer, T.; Gast, P.; Jeschke, G.; Alia, A.; Matysik, J. *Biochemistry* **2008,** *47*, 4629. doi: 10.1021/bi800030g

(11) Alia; Roy, E.; Gast, P.; van Gorkom, H. J.; de Groot, H. J. M.; Jeschke, G.; Matysik, J. *J. Am. Chem. Soc.* **2004,** *126*, 12819.

(12) Diller, A.; Roy, E.; Gast, P.; van Gorkom, H. J.; de Groot, H. J. M.; Glaubitz, C.; Jeschke, G.; Matysik, J.; Alia, A. *Proc. Natl. Acad. Sci. U. S. A.* **2007,** *104*, 12767. doi: 10.1073/pnas.0701763104

(13) Matysik, J.; Diller, A.; Roy, E.; Alia, A. *Photosynth. Res.* **2009,** *102*, 427. doi: 10.1007/s11120-009-9403-9

(14) Hoff, A. J.; Deisenhofer, J. *Phys. Rep.* **1997,** *287*, 2.

(15) Hunter, C. N.; Daldal, F.; Thurnauer, M. C.; Beatty, J. T. *The Phototropic Purple Bacteria*; Springer: Dordrecht, The Netherlands, 2008.

(16) Thamarath, S. S.; Bode, B. E.; Prakash, S.; Karthick, B. S. S. G.; Alia, A.; Jeschke, G.; Matysik, J. *J. Am. Chem. Soc.* **2012,** *134*, 5921. doi: 10.1021/ja2117377

(17) Thamarath, S. S.; Heberle, J.; Hore, P.; Kottke, T.; Matysik, J. *J. Am. Chem. Soc.* **2010,** *132*, 15542. doi: 10.1021/ja1082969

(18) Hore, P. J.; Hunter, D. A.; McKie, C. D.; Hoff, A. J. *Chem. Phys. Lett.* **1987,** *137*, 495. doi: 10.1016/0009-2614(87)80617-6

(19) Closs, G. L.; Closs, L. E. *J. Am. Chem. Soc.* **1969,** *91*, 4549. doi: 10.1021/ja01044a041

(20) Kaptein, R.; Oosterhoff, J. L. *Chem. Phys. Lett.* **1969,** *4*, 195. doi: 10.1016/0009-2614(69)80098-9

(21) Wirtz, A. C.; van Hemert, M. C.; Lugtenburg, J.; Frank, H. A.; Groenen, E. J. J. *Biophys. J.* **2007,** *93*, 981. doi: 10.1529/biophysj.106.103473

(22) Daviso, E.; Jeschke, G.; Matysik, J. *J. Phys. Chem. C* **2009,** *113*, 10269. doi: 10.1021/jp900286q

(23) Jeschke, G. *J. Chem. Phys.* **1997,** *106*, 10072. doi: 10.1063/1.474063

(24) Jeschke, G. *J. Am. Chem. Soc.* **1998,** *120*, 4425.

(25) Polenova, T.; McDermott, A. E. *J. Phys. Chem. B* **1999,** *103*, 535. doi: 10.1021/jp9822642

(26) Diller, A.; Prakash, S.; Alia, A.; Gast, P.; Matysik, J.; Jeschke, G. *J. Phys. Chem. B* **2007,** *111*, 10606. doi: 10.1021/jp072428r

(27) Jeschke, G.; Matysik, J. *Chem. Phys.* **2003,** *294*, 239. doi: 10.1016/S0301-0104(03)00278-7

(28) McDermott, A.; Zysmilich, M. G.; Polenova, T. *Solid State Nucl. Magn. Reson.* **1998,** *11*, 21. doi: 10.1016/S0926-2040(97)00094-5

(29) Closs, G. L. *Chem. Phys. Lett.* **1975,** *32*, 277. doi: 10.1016/0009-2614(75)85123-2

(30) Goldstein, R. A.; Boxer, S. G. *Biophys. J.* **1987,** *51*, 937. doi: 10.1016/S0006-3495(87)83421-5

(31) Wang, X. J.; Thamarath, S. S.; Matysik, J. *Acta Chim. Sin.* **2013,** *71*, 169. [王孝杰, Thamarath, S. S., Matysik, J. 化学学报, **2013,** *71*, 169.] doi: 10.6023/A12121093

(32) Jeschke, G.; Anger, B. C.; Bode, B. E.; Matysik, J. *J. Phys. Chem. A* **2011,** *115*, 9919. doi: 10.1021/jp204921q

(33) Wang, J.; Du, X. L.; Pan, W. S.; Wang, X. J.; Wu, W. J. *J. Photochem. Photobiol. C* **2015,** 22, 84. doi: 10.1016/j.jphotochemrev.2014.12.001

(34) Chaves, I.; Pokorny, R.; Byrdin, M.; Hoang, N.; Ritz, T.; Brettel, K.; Essen, L. O.; van der Horst, G. T. J.; Batschauer, A.; Ahmad, M. *Annu. Rev. Plant Biol.* **2011,** *62*, 335. doi: 10.1146/annurev-arplant-042110-103759